Chemical Science

ROYAL SOCIETY OF CHEMISTRY

EDGE ARTICLE

View Article Online
View Journal | View Issue

Cite this: *Chem. Sci.*, 2023, **14**, 2721

All publication charges for this article have been paid for by the Royal Society of Chemistry

Inexpensive and bench stable diarylmethylium tetrafluoroborates as organocatalysts in the light mediated hydrosulfonylation of unactivated alkenes†

Polyssena Renzi, Emanuele Azzi, Sylvain Ascensio, Stefano Parisotto, Fabrizio Sordello, Francesco Pellegrino, Giovanni Ghigo * and Annamaria Deagostino *

Received 11th January 2023
Accepted 10th February 2023

DOI: 10.1039/d3sc00182b

rsc.li/chemical-science

In this paper, we present the synthetic potential of diarylmethylium tetrafluoroborates as catalysts for the visible light promoted hydrosulfonylation of unactivated alkenes. For the first time, these salts, which are bench stable and easily preparable on a multi-gram scale, were employed as organocatalysts. Interestingly, a catalyst loading of only 1 mol% allowed sulfone products to be efficiently obtained from good-to-excellent yields with high functional-group tolerance and scalability up to 15 mmol of alkene. The mechanistic study, both experimental and computational, presented here, revealed an alternative mechanism for the formation of the key sulfonyl radical. Indeed, the photoactive species was proved not to be the diarylcarbenium salt itself, but two intermediates, a stable S–C adduct and an ion couple, that were formed after its interaction with sodium benzenesulfinate. Upon absorbing light, the ion couple could reach an excited state with a charge-transfer character which gave the fundamental sulfonyl radical. A PCET (proton-coupled electron transfer) closes the catalytic cycle reforming the diarylcarbenium salt.

Introduction

Sulfones are privileged building blocks for medicinal chemistry, drug discovery and natural-product synthesis,[1,2] therefore, the search for operationally simple and easily scalable methodologies for their preparation is a current hot topic.[3,4] To overcome the drawbacks associated with the traditional oxidation of sulfides or sulfoxides,[5–8] considerable effort has been devoted to the development of SO_2 surrogates,[9–11] and to the employment of alternative solvents (water, deep eutectic solvents, and solvent free).[12,13] Moreover, emerging techniques such as photochemistry[14,15] and electrochemistry are increasingly gaining ground.[12] In most cases, the key step to the success of these reactions is the generation of the sulfonyl radical from suitable precursors (*e.g.* sodium sulfinates, sulfonyl chlorides, sulfinic acids, sulfonyl hydrazides, sulfonyl imines, and DABCO$(SO_2)_2$).[16–20] Vicinal difunctionalisation is generally observed under photocatalysis[21–24] when feedstock chemicals, such as alkenes, are employed as coupling partners, while methods enabling their direct hydrosulfonylation are very limited. The first example was reported by Yu in 2019 (Scheme 1a).[25] The anti-Markovnikov hydrosulfonylation of alkenes bearing alkyl groups was accomplished under iridium-photocatalysis in the presence of sodium sulfinates, used as sulfonyl radical precursors. This methodology has also been applied to electron-poor alkenes showing reduced reactivity and/or the formation of product mixtures. In 2020, Liu and Duan applied the protocol to styrenes by substituting acetic acid and water with methanol for use as a proton source (Scheme 1b).[26] Pre-activated sulfone tetrazoles, and activated sulfonyl chlorides were also proposed as sulfonyl radical precursors by Ley[27] and Gouverneur.[28] In the first case, acrylates and electron-poor alkenes can be readily converted to dialkyl sulfones under iridium photoredox catalysis. The success of this protocol is somewhat tempered by the need for a stoichiometric amount of DMAP as a sacrificial reagent, and $Cu(OAc)_2$ as an external oxidant (Scheme 1c). In the second case, sulfonyl chlorides are employed for the hydrosulfonylation of electron-deficient alkenes under visible light activation for the first time. However, the use of $(TMS)_3$-SiH as a H donor is necessary. In this way, they have developed a mild protocol that is suitable for late-stage functionalisation (Scheme 1d).

Department of Chemistry, University of Torino, Via Pietro Giuria, 7, 10125 Torino, Italy. E-mail: deagostino.annamaria@unito.it; giovanni.ghigo@unito.it

† Electronic supplementary information (ESI) available: Additional experimental details, materials, and methods, including photographs of the experimental setup and NMR spectra of all compounds (PDF). Details of the computational method, additional discussions and figures, table with absolute and relative energies, pictures of all structures (with imaginary frequencies for the TSs) and relative Cartesian coordinates (PDF). See DOI: https://doi.org/10.1039/d3sc00182b

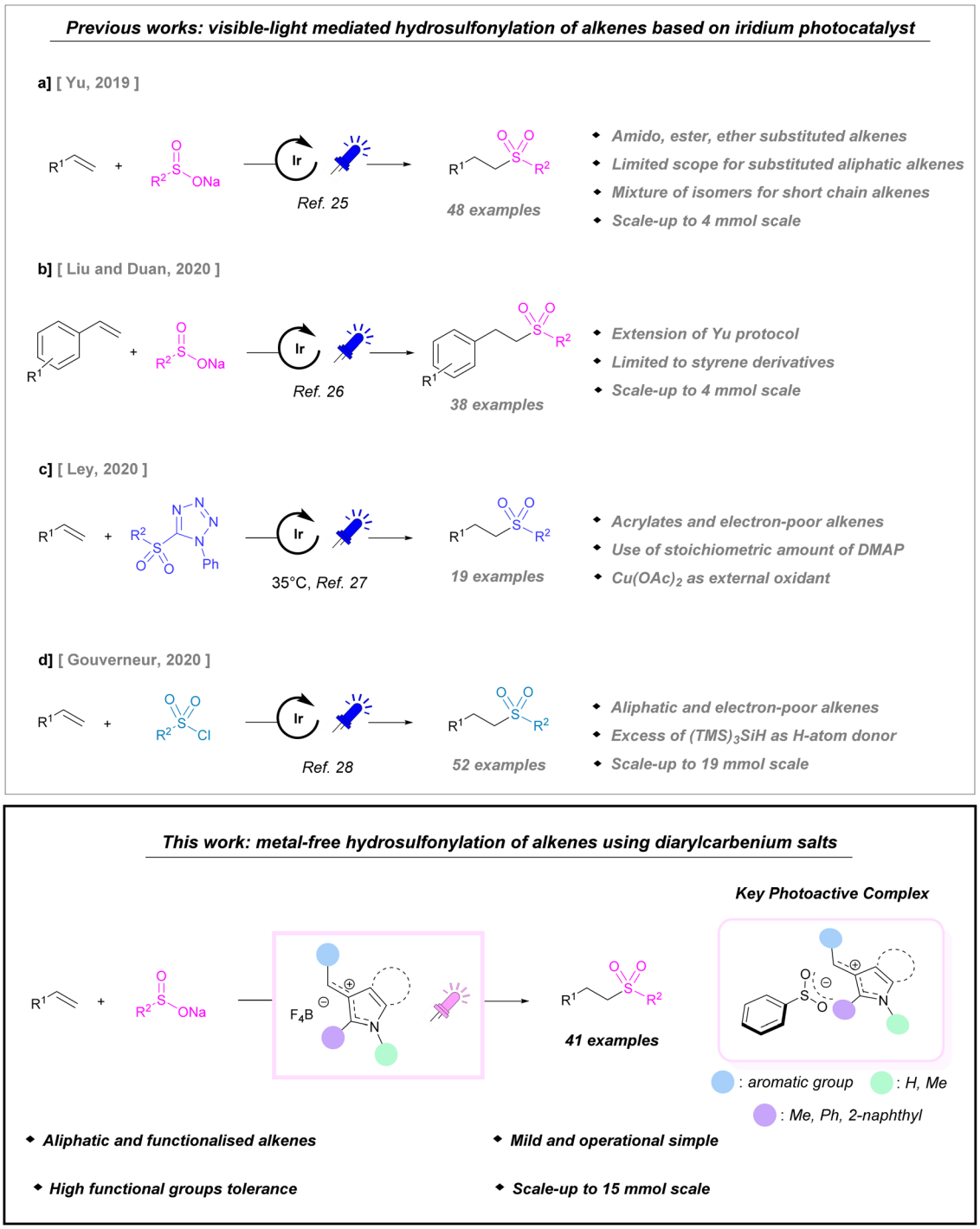

Scheme 1 Top: previously reported visible-light hydrosulfonylation of alkenes; bottom: this work.

More recently, Xue and Luo have reported the use of sulfonyl imines as versatile sulfonyl precursors under iridium/copper dual catalysis.[20] As shown in Scheme 1, the hydrosulfonylation of alkenes mediated by visible light is dominated by iridium catalysis. Although polypyridyl complexes of iridium are robust photocatalysts, they can be acid sensitive[29] and the low abundancy of this metal[30] makes these compounds unsustainable from economic and environmental points of view. Moreover, their high costs potentially limit their application on industrial scale. While iridium and ruthenium complexes still stand at the forefront of photocatalysis, in recent years, organic dyes (*e.g.* acridinium salts, anthraquinones, Eosin Y, cyanoarenes, *etc.*) have emerged as a sustainable option due to their stability, photocatalytic performances and wide range of useful redox potentials.[31–36]

As part of our ongoing research on the photocatalyzed functionalisation of unsaturated compounds,[37–39] we have developed an operationally simple anti-Markovnikov

hydrosulfonylation of a broad range of unactivated alkenes **1** with sodium sulfinates **2a–e** in the presence of diarylmethylium tetrafluoroborates under purple light (Scheme 1, bottom). This class of compounds is known in the literature as a model substrate in organocatalyzed alkylation reactions[40–43] or together with benzhydrylium ions have been employed by Mayr as reference electrophiles for the construction of a general basicity scale.[44,45] For the first time, we have employed non-symmetric diarylcarbenium salts **I–XII** as organocatalysts in a light mediated process. These salts strongly absorb in the visible spectrum, with absorption maxima ranging from red to yellow according to their substitution patterns. They can be easily synthesised on the gram scale *via* the direct condensation of aryl or heteroaryl aldehydes and *N*-heteroarenes. Interestingly, they are bench-stable salts with long shelf life and high stability, embodying the characteristics of the ideal catalyst. Furthermore, their structure can be easily modulated to finely tune their redox potentials. An additional aspect that should not be underestimated is the catalyst cost as diarylcarbenium salts are more economically viable than iridium catalysts.[46]

Results and discussion

We initiated our study by evaluating the spectroscopic and electrochemical properties of several diarylcarbenium tetrafluoborates **I–XII**, which were available in our laboratory (for full characterization see Table S7 in the ESI†). Cyclic voltammetry (CV) measurements showed an interesting match between the redox potentials of salts **I–XII** and sodium benzenesulfinate **2a**, which suggested their potential application as a catalyst in the hydrosulfonylation of unsaturated compounds. Therefore, hexadec-1-ene **1a** and sodium benzenesulfinate **2a** were chosen as the model substrates to prove our hypothesis, starting from reaction conditions reported by Yu.[25] The reaction was not feasible at room temperature, at 40 °C or under illumination at 525 nm (Table 1 entries 2–3) in the presence of tetrafluoroborate salt **I** (10 mol%), water (10 eq.) and acetic acid (4.5 eq.) in CH_2Cl_2, whereas product **3a** was isolated in a 22% yield under illumination with a 40W Kessil blue LED lamp (Table 1 entry 4). Unsatisfactory results were obtained under all the conditions tested at 456 nm (for the complete set of experiments see Table S1†). This observation and the lack of reactivity under green light can be rationalized by the colour bleaching of diarylcarbenium **I** when sulfinate **2a** was added to the reaction medium, which hints at there being a different active species than **I** in this light-mediated process.

Therefore, we tested the hydrosulfonylation under purple LED lamp irradiation (390 nm) and we were delighted to observe a 71% yield of **3a** in the presence of 10 mol% of **I** (Table 1 entry 5). As described in Table 1 entry 6, a decrease in the catalyst amount, from 10 to 5 mol%, was beneficial to the reaction outcome with an increase in yield up to 87%. A further reduction in **I**, loading at 3 mol%, caused a slight decrease to an 83% yield (Table 1 entry 7). Interestingly, the use of only 1 mol% of salt **I** still resulted in an 80% yield (Table 1 entry 1). We consider this to be the most convenient result because a high yield was obtained with a very low loading of **I**, which is an organocatalyst. Moreover, this amount corresponds to the catalyst loading generally used in iridium photocatalysis in similar reactions.[25,26] We therefore decided to continue our optimization with 1 mol% of **I**. We also confirmed a lack of reactivity under illumination with a 390 nm LED lamp in the absence of the diarylcarbenium salt **I** (Table 1 entry 8).

Then, reaction conditions were extensively screened in order to assess the role of the solvent, acid, water and sulfinate amount (see the ESI† for exhaustive Tables). Regarding the solvent, the protic $CHCl_3$ and the aprotic THF were less efficient than CH_2Cl_2 both affording the product with a 50% yield (Table 1 entries 9–10). The use of CH_3CN caused a further drop to a 30% yield (Table 1 entry 11). Other solvents such as DMF or 2-Me-THF proved to be very inefficient (see Table S3†). A dilution of the reaction mixture from 0.2 M to 0.1 M in CH_2Cl_2 was not beneficial, resulting in a 64% yield of **3a** (Table 1 entry 12).

The reaction outcome was highly dependent on the presence of the acid and water with a complete lack of reactivity in the absence of both (Table 1 entries 13 and 16). Organic acids such as formic and acetic acid (Table 1 entries 14 and 1, respectively 77 and 80%) performed better than inorganic acids, the latter causing the degradation of alkene **1a** (for the complete screening see Tables S4 and S5†). A screening of the equivalents of acetic acid was also accomplished, showing the need for an excess of this acid. As reported in entry 15 of Table 1, the use of a stoichiometric amount of acetic acid decreased the yield to 41% (*versus* 80% yield with 4.5 eq. of acetic acid). An excess of water was necessary, in order to assure the best solubility of sodium benzenesulfinate **2a**. Best results were obtained with 10 equivalents as shown in Table 1 entry 1. Higher or lower amounts resulted in a slight decrease in the reaction efficiency, a 66% and 72% yield for **3a** were respectively observed with 6 and 20 equivalents of water (Table 1 entries 17–18, see also Table S5†). Our attention was then pointed towards the influence of the sodium benzenesulfinate **2a** amount with respect to hexadec-1-ene **1a**. Neither the use of 1.1 (59%, Table 1 entry 19) or 3 equivalents of **2a** (70%, entry 20) resulted to be beneficial in comparison to the starting 1.6 equivalents.

We next sought to evaluate the catalyst structure changing the aryl moiety and the substituents on C2 and nitrogen of the indole portion of the diarylcarbenium salt. A selection of the results is reported in Table 1b, whereas the complete study is described in Table S7 of the ESI.† According to the substitution patterns, the diarylcarbenium salts **I–XII** showed a different efficiency in promoting the hydrosulfonylation of hexadec-1-ene **1a** with **2a**. Several tetrafluoroborates were prepared and the effect of the substituents at C2 and N of the indole core was evaluated. In general, from good to high yields were obtained with diarylcarbenium salts **I–IV**, bearing a methoxy-naphthyl moiety and a *N*-methyl indole. A moderate decrease in yield from 80 to 66% was observed increasing the size of the substituent at C2 of the indole portion while keeping the 2-methoxynaphthyl moiety (Table 1b, **I** and **IV**). A dramatic drop in the efficiency was achieved for those catalysts derived from a substituted benzaldehyde and 2-methylindole (Table 1b, **VIII** and **X**). Therefore, the presence of a methylated nitrogen proved

to be essential for high yield except for compound **V** which despite being a N–H salt gave a 70% yield for **3a** (Table 1b).

Although most diarylcarbenium tetrafluoborate salts showed discrete to good efficiency, no direct correlation could be found with their electronic properties and redox potentials. As shown in Table 1b, tetrafluoroborate salts with similar redox potentials, *e.g.* **I** and **X** or **V** and **VIII**, gave very different yields in the hydrosulfonylation of hexadec-1-ene **1a**. Therefore, we became suspicious of the role of diarylmethylium tetrafluoborates as effective catalysts in this transformation. We must recall also the colour bleaching observed upon the addition of **2a**. Mechanistic studies were then initiated in order to understand the actual catalytic species involved here.

In summary, the complete screening of catalysts, reagent amounts and ratios (fully described in the ESI†) confirmed the conditions reported in Table 1 entry 1 to be the optimal. Thus, a simple setup composed of 1 mol% of salt **I**, 4.5 equivalents of acetic acid and 10 equivalents of water in CH_2Cl_2 under irradiation with a purple LED lamp at room temperature enabled

Table 1 Optimization of the reaction conditions for the anti-Markovnikov hydrosulfonylation – selected results

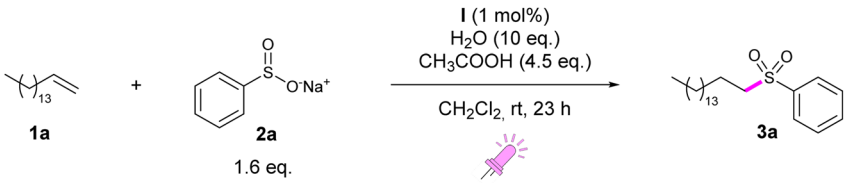

a. Optimisation of the reaction conditions

Entry	Deviation	**3a** Yield [%][b]
1	**None**[a]	**80**
2	No irradiation at rt or 40 °C	0
3	Green LED lamp (525 nm)	0
4	Blue LED lamp (456 nm)	22[c]
5	**I** (10 mol%)	71
6	**I** (5 mol%)	87
7	**I** (3 mol%)	83
8	No **I**	0
9	$CHCl_3$ as solvent	50
10	THF as solvent	50
11	CH_3CN as solvent	30
12	0.1 M in CH_2Cl_2	64
13	No acid	Traces
14	HCOOH as acid	77
15	1 eq. of CH_3COOH as acid	41
16	No H_2O	0
17	H_2O (6 eq.)	66
18	H_2O(20 eq.)	72
19	**2a** (1.1 eq.)	59
20	**2a** (3 eq.)	70

b. Screening of selected diarylmethylium tetrafluoroborates salts

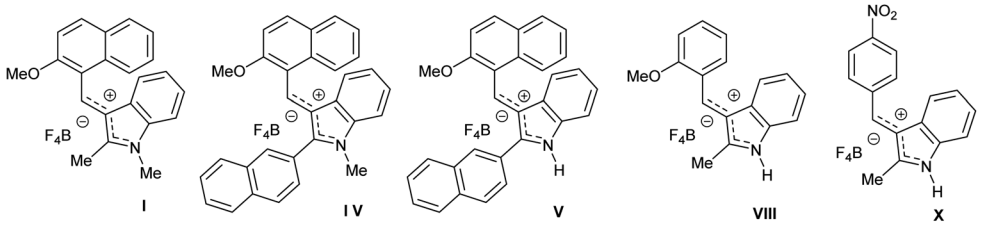

	I	IV	V	VIII	X
λ_{max}	522 nm	543 nm	533 nm	446 nm	392 nm
E^0	-0.395 V	-0.275 V	-0.480 V	-0.490 V	-0.380 V
Yield **3a**	80%	66%	70%	2%	35%

[a] Reaction conditions: hexadec-1-ene **1a** (0.5 mmol), sodium benzenesulfinate **2a** (0.8 mmol, 1.6 eq.), **I–XII** (1 mol%), in CH_2Cl_2 (2.5 mL; 0.2 M), CH_3COOH (2.25 mmol, 4.5 eq.), H_2O (5 mmol, 10 eq.), 40W Kessil purple LED lamp (390 nm), 23 h, room temperature. [b] Determined on the isolated product. [c] Carried out with 10% mol of **I**.

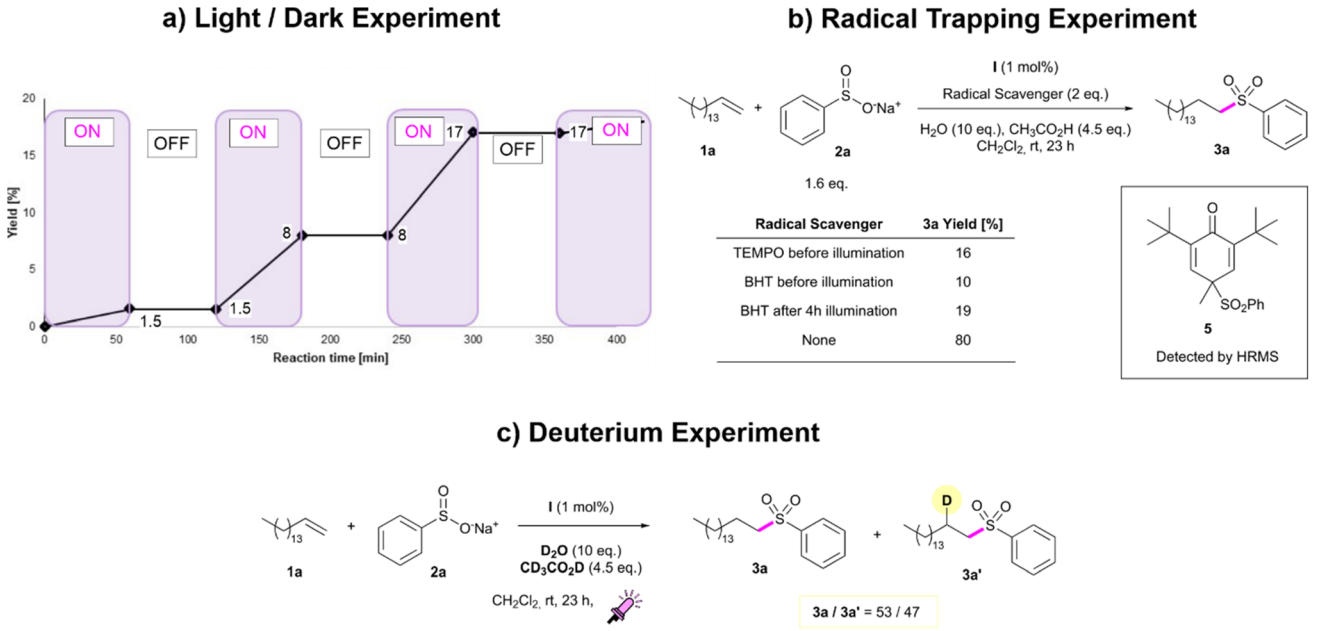

Fig. 1 a) The light/dark experiment. (b) The TEMPO/BHT trapping experiment. (c) The deuterium experiment. The details of the experimental conditions for each study are reported in the ESI.†

an efficient anti-Markovnikov functionalisation of alkene **1a** to afford sulfone **3a**.

Mechanistic studies: experimental and computation

Experimental mechanistic studies

In order to understand the function of purple light in the hydrosulfonylation of alkenes, we turned our attention to the reaction mechanism. The crucial role of light was demonstrated by a light/dark experiment which showed reaction progression solely under irradiation (Fig. 1a). Then, to gain further insight into the reaction mechanism and prove the formation of radical intermediates, we performed trapping experiments with 2,2,6,6-tetramethyl-1-piperidinyloxy (TEMPO) and butylhydroxytoluene (BHT) as radical scavengers (Fig. 1b). When 2 equivalents of TEMPO were added to the reaction mixture under standard conditions, the transformation efficiency drastically dropped (16% yield *vs.* 80% under standard conditions for **3a**). In the presence of the radical scavenger BHT, the yield of the sulfonylation product **3a** further dropped to 10% suggesting that a radical pathway could be involved in this transformation (Fig. 1b). This idea was additionally confirmed by the detection of the BHT-sulfonyl radical adduct **5** by HRMS. Furthermore, when the reaction was carried out under an O_2 atmosphere, no product formation was observed. The reaction proceeded with an anti-Markonikov selectivity in which acetic acid played a crucial role, as shown in the optimisation. Moreover, deuterium experiments showed the introduction of deuterium into the β-position of sulfone **3a**. The deuterated product **3a′** was obtained along with its non-deuterated counterpart **3a** in 47/53 ratio in the presence of CD_3COOD and D_2O (Fig. 1c).

Determination of the catalytic species

In order to determine the actual catalytic species, we performed the UV-vis analysis of diarylmethylium salt **I** alone and in the presence of sodium benzenesulfinate **2a**. As shown in Fig. 2a, salt **I** is a bright coral red solid showing two absorption bands centered at 522 (visible) and 382 (UV-A) nm (black line in **2a**) in CH_2Cl_2. When sodium benzenesulfinate **2a** is added to **I** solution, a fast and progressive colour fading to colourless is observed together with the complete suppression of both characteristic absorption bands of the diarylmethylium tetrafluoroborate salt **I** (red line in Fig. 2a) and the appearance of a new band in the UV-B region (black line in Fig. 2a). This fact, as pointed out in the reaction optimisation, made us suspect that the catalytic species in this transformation might not be the diarylmethylium salt itself. To better understand the interactions existing between **I** and the sulfinate **2a**, we performed ^{1}H-NMR analysis of a 1/1 mixture of **I**/**2a** in CD_2Cl_2. Ten equivalents of D_2O were added to improve sulfinate solubility. As displayed in Fig. 2c, the singlet centred at 9.01 ppm, pertinent to the methenyl (C^{10}–H) between the naphthyl and indolyl moieties of **I**, disappeared. Moreover, the C^2–CH_3 was shielded and the corresponding singlet was shifted by 0.88 ppm. The signals at 3.55, 6.82, and 8.01 ppm were subjected not only to a shift but also to a broadening indicating a direct interaction between **I** and sulfinate **2a**.

Cyclic voltammetry (CV) demonstrated that the diarylmethylium salts have an irreversible reduction peak at −0.5 V *vs.* Ag/AgCl as the most distinguishable redox feature (Fig. 2b and ESI†). In the case of **I**, this characteristic peak disappeared in the first cycle in the presence of sulfinate **2a** (Fig. 2b). Moreover, when subjected to repeated cycles, its current was significantly reduced (ESI†). In contrast, this characteristic peak

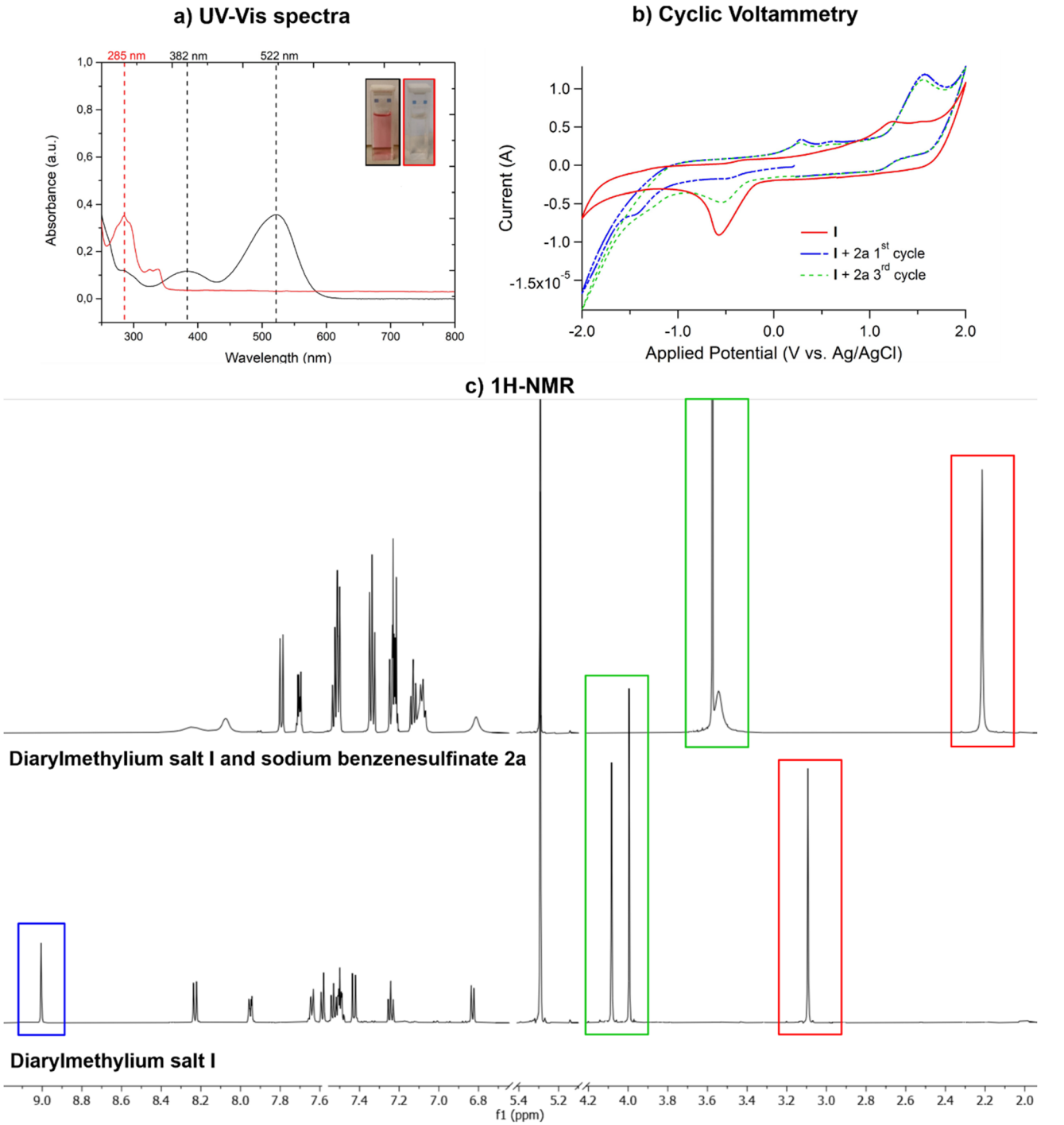

Fig. 2 (a) UV-vis spectra of diarylcarbenium salt **I** (20 mM) in CH_2Cl_2 before (black line) and after (red line) the addition of sodium benzenesulfinate **2a**. (b) CV recorded in CH_2Cl_2 at 200 mV s^{-1} of **I** with and without an excess of **2a**. (c) Comparison between the ^{1}H-NMR (600 MHz) spectra of salt **I** alone (bottom) and in the presence of **2a** (top) in CD_2Cl_2 with 10 equivalents of D_2O.

completely disappeared for the diarylmethylium salts not showing a good catalytic activity in the hydrosulfonylation. (see the ESI†). The anodic current peaks observed in the presence of sulfinate **2a** were assigned to the sulfinate moiety (Fig. 2b), because very similar features were observed when sulfinate **2a** alone was dissolved in methanol (Fig. S26 in the ESI†). Conversely, sulfinate **2a** did not give redox features in CH_2Cl_2, due to its scarce solubility. Therefore, we hypothesized that sulfinate **2a** and diarylmethylium salts might form an adduct increasing the solubility of sulfinate in CH_2Cl_2. Moreover, the adduct should have a charge-transfer nature, as witnessed by the changes in the current of the cathodic peak and in both current and potential of the anodic peaks assigned to the sulfinate moiety (Fig. 2b and ESI†). Therefore, to clarify the

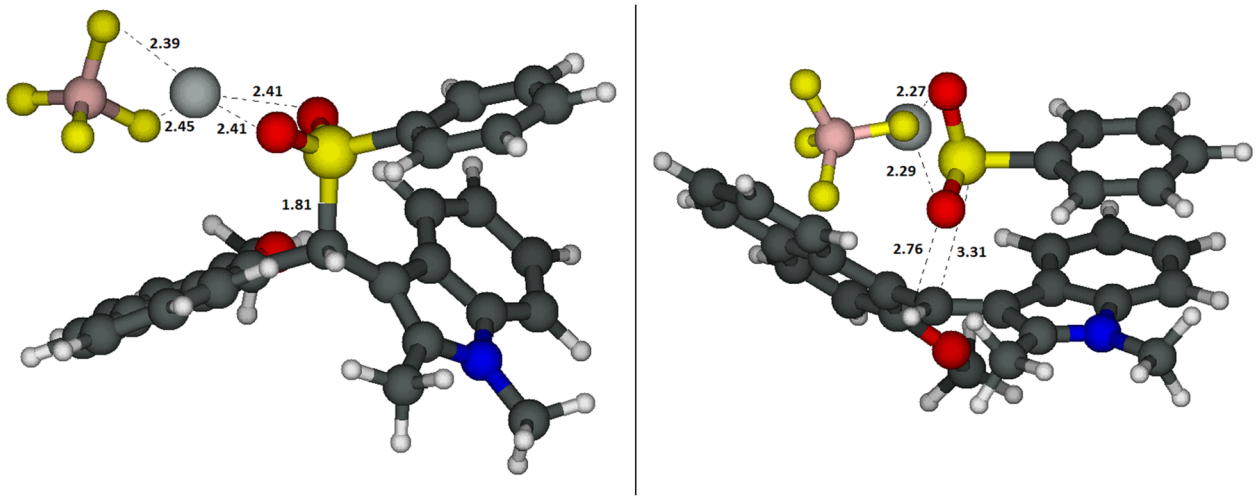

Fig. 3 Structures of the S–C bound adducts **AD** (left) and the complex **A** between sodium benzenesulfinate **2a** and the catalyst **I** (right). Color code: black = carbon, white = hydrogen, blue = nitrogen, red = oxygen, yellow = sulfur. The distances are in Ångström.

interactions between the catalyst and the sulfinate, quantum chemical calculations were carried out.

Computational study

Computational studies were performed on pent-1-ene **1d** as the model alkene, tetrafluoroborate **I** (hereafter, indolynium $\mathbf{I}^{+}$) as the catalyst and acetic acid as the co-reactant and co-catalyst. The analysis of the different configurations and conformations (Tables S-1a/b†) and the electronic structure (group charges and LUMO, Fig. S-1†) of the catalyst **I** are reported in the ESI-Computational Data (ESI-CD†). In discrete agreement with the experimental findings, the first active electronic transition for catalyst **I** was calculated using time-dependent density functional theory (TD-DFT) at 484–494 nm (*versus* the experimental 522 nm, see Fig. 2a). It corresponds to the transition from the HOMO, mainly localized on the naphthyl moiety, to the LUMO orbital, mainly situated on the indolynium unit (see Fig. S-2 in the ESI-CD†). For the mixture catalyst **I**/sodium benzenesulfinate **2a**, calculations predicted the formation of two intermediates in equilibrium between themselves (ESI-CD, Table S-2a†). The most stable is an S–C adduct **AD**, where the sulphur is directly bound to the methenyl carbon C^{10}–H (Fig. 3, left).

This adduct is 9.8 kcal mol^{-1} more stable than the separated species in terms of free energy. In agreement with the experimental findings, the calculated first electronic transition at 358 nm for adduct **AD** matched the lack of absorbance in the visible region observed when **I** and **2a** are mixed together (see Fig. 2a for the experimental UV-vis spectrum). The electronic structure of the first excited state (Fig. S-3, ESI-CD†) is mainly described by a transition that involves π and π* orbitals localized on the three aromatic moieties. The contributions of the SO_2 moiety and of the σ_{CS}* (essential for the dissociation of this bond) are negligible. This, along with the fact that **AD** does not absorb in the visible, should exclude the creation of the radical couple by photodissociation of the C–S bound adduct. Moreover, the calculated ^{1}H-NMR isotropic magnetic shielding tensors were qualitatively coherent with the experimental findings (Fig. 2c) with a calculated shift for most hydrogen atoms between −1.5 and +0.5 ppm going from **I** to the S–C adduct **AD**. The highest upshift of +3.2 ppm was calculated for the C^{10}–H.

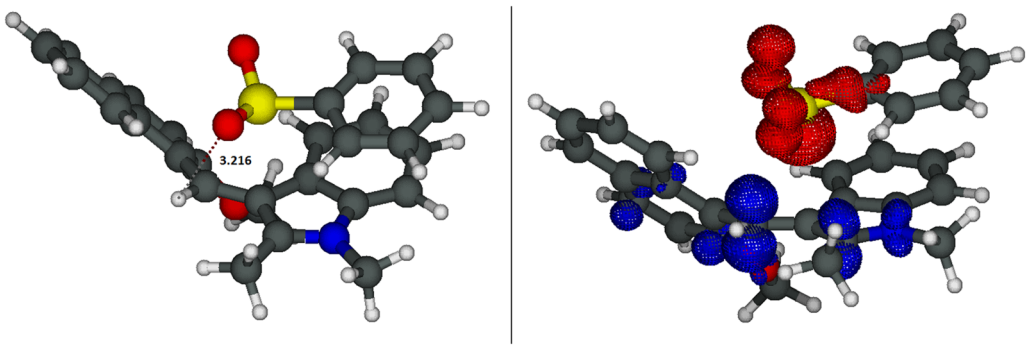

Fig. 4 Structure of the first excited state S_1-A′* of the complex A′ between sodium benzenesulfinate $\mathbf{2a}^{-}$ and indolynium $\mathbf{I}^{+}$ (left) and differential density map (right, the red areas correspond to a reduction in the electronic density when going from S_0 to S_1, and the blue areas correspond to an increase in the electronic density). Color code: black = carbon, white = hydrogen, blue = nitrogen, red = oxygen, yellow = sulfur. The distances are in Ångström.

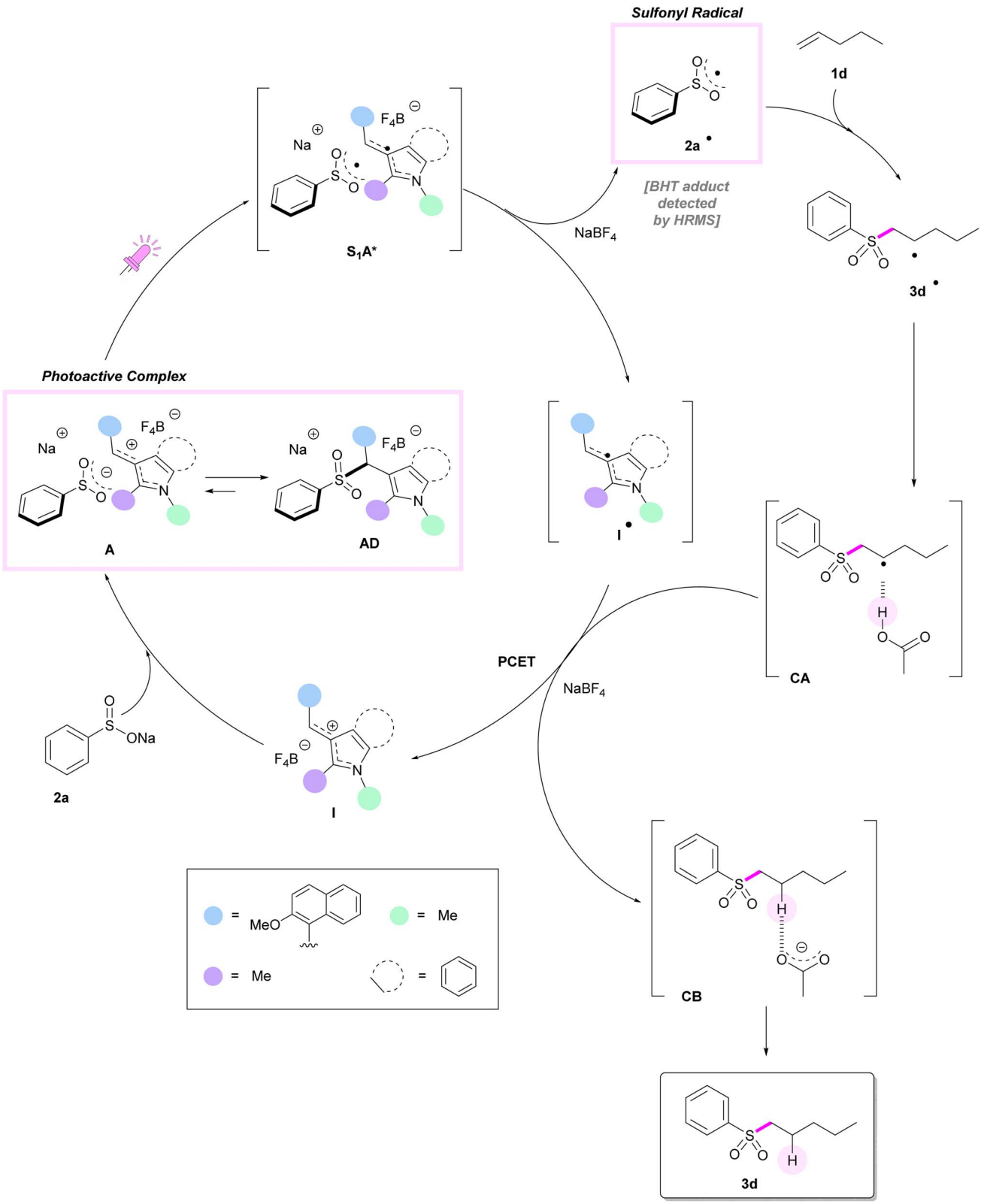

Scheme 2 Proposed full reaction mechanism.

As shown in Fig. 3 right, the second species is the complex **A**, an ion couple formed between **2a** and **I** characterized by a hydrogen bond between the C^{10}–H and one of the oxygens of the sulfinate **2a**. This complex is located 7.4 kcal mol^{-1} below the reactants, but only 2.5 kcal mol^{-1} above the S–C adduct **AD**. Therefore, according to our calculations the covalent adduct **AD** should be the prevailing species, while very small concentrations (*ca.* 2%) of complex **A** are present in solution. A similar

case was, recently, reported by the Gaunt group.[47] Despite the low amount of complex **A**, it is the key reactive species. Indeed, as indicated by the TD-DFT calculations, its first excited state S_1 showed a charge-transfer character that can prelude to the generation of a couple of radicals, *i.e.* the phenyl sulfonyl radical **2a**$^{\bullet}$ and the indolyl radical **I**$^{\bullet}$. In fact, this S_1 state corresponds to an electronic transition from the HOMO localized on the anionic SO_2^- moiety to the LUMO localized on the indolinium **I**$^+$ (see Fig. S-4a in the ESI-CD†). To simplify the model (and to solve the problems of convergence in the optimisation of the first excited state with the TD-DFT calculations, data in Table S-2b, ESI-CD†), we optimised the structures of the complex between the indolyl cation **I**$^+$ and the sodium benzenesulfinate **2a**$^-$ without their counter-ions (*i.e.* Na^+ and BF_4^-). The structure of this new complex, **A**′ (Fig. S-4b in the ESI-CD†) is similar to that with the counterions and its first excited state also showed the same charge-transfer character (*i.e.* a transition from the HOMO localized on the anionic SO_2^- moiety to the LUMO localized on the indolinium **I**$^+$, see Fig. S-4c in the ESI-CD†). The optimisation of the structure of the first excited state of complex **A**′ leads to **S$_1$-A**′* (Fig. 4, left) which is located, in terms of electronic energy (ΔE^{TZ}, free energies are not available at the TD-DFT level) 32.7 kcal mol^{-1} above **A**, but only 16.8 kcal mol^{-1} with respect to the separated ions **2a**$^-$ and **I**$^+$. Also **S$_1$-A*** shows an electronic structure corresponding to the couple of radicals formed by the phenylsulfonyl **2a** and the indolyl radical **I**$^{\bullet}$. This can also be deduced from the differential density map reported in Fig. 4, right and from the group charges (Fig. S-5 in the ESI-CD†). Therefore, we hypothesized that, upon irradiation, the carbocation **I**$^+$ is able to reduce itself to the radical **I**$^{\bullet}$, thus oxidizing **2a**$^-$ to the sulfonyl radical **2a**$^{\bullet}$ once the complex **A**$^-$ is formed (Scheme 2). The formation of **2a**$^{\bullet}$ was also confirmed by a trapping experiment with BHT (Fig. 1b). We want to underline that, as experimentally found, this redox reaction is not spontaneous but it requires light to take place.

S$_1$-A′* can decay to the original **A**′ or to its corresponding triplet states **T$_1$-A**′, located 16.1 kcal mol^{-1} above **2a**$^-$ and **I**$^+$ in terms of free energy (but 10.1 kcal mol^{-1} below **S$_1$-A**′* in terms of electronic energy). Both **S$_1$-A**′* and **T$_1$-A**′ can dissociate into the separated radicals **2a**$^{\bullet}$ and **I**$^{\bullet}$ which are located 15.0 kcal mol^{-1} above the ions in terms of free energy, but 1.1 kcal mol^{-1} below **T$_1$-A**′ and *c.a.* 11.2 kcal mol^{-1} below **S$_1$-A**′* (assuming the same thermal correction as for the triplet state which is structurally and electronically similar to the first excited singlet state).

As described in Scheme 2, once generated, the radical **2a**$^{\bullet}$ can add to the alkene **1d** to yield intermediate **3d**$^{\bullet}$ which is a secondary radical and the precursor of the product. Its formation is quite fast ($\Delta G^{\ddagger}$ = 10.8 kcal mol^{-1}, k = 1.8 10^6 M^{-1} s^{-1}), but thermodynamically slightly disfavoured (ΔG = 1.3 kcal mol^{-1}). The reduction of the radical intermediate **3d**$^{\bullet}$ by the reduced indolyl radical **I**$^{\bullet}$ followed by protonation by acetic acid yielding the final product is thermodynamically favoured (ΔG = −19.1 kcal mol^{-1}), but the process seems to be more complicated. As itself, the reduction of the radical **3d**$^{\bullet}$ by the oxidation of the radical **I**$^{\bullet}$ to regenerate the carbocation catalyst **I**$^+$ is thermodynamically disfavoured (the estimated value by single point calculation is ΔE^{TZ} = 32.7 kcal mol^{-1}). Moreover, the anionic state of **3d**$^{\bullet}$ is not stable and spontaneously breaks into the starting reactants. However, if one considers the structure of **CA** between radical **3d**$^{\bullet}$ and acetic acid and its re-optimised structure after reduction (*i.e.* **CA** as an anion), a proton transfer spontaneously takes place yielding **CB** between the final product **3d** and acetate which is located 23.1 kcal mol^{-1} below the starting **CA** in terms of energy (ΔE^{TZ}, see Fig. S-6 in the ESI-CD†). The final **CB** is 20.8 kcal mol^{-1} below **CA** in terms of free energy. Therefore, in our hypothesis, the reduction and proton transfer can take place in a sort of proton-coupled-electron-transfer, PCET.[48–51] The favourable energetics related to the proton transfer step, in fact, compensates the unfavourable energetics of the electron transfer event. In particular, this case could be classified as a reductive multiple-site PCET,[52] where the interaction between the carbon radical and the acid could be favoured by the high concentration of the latter *in lieu* of the molecular structure of the reactant. In our case, the employment of higher than stoichiometric concentrations of acid and the result of the incorporation of deuterium are coherent with this PCET mechanism. Therefore, the acid can induce the reduction of the radical intermediate **2a**$^{\bullet}$ yielding the thermodynamically stable products. A final counter-ion recombination yields product **3d**, sodium acetate and the regenerated catalyst **I** (ΔG = −22.2 kcal mol^{-1}). The whole reaction is only slightly thermodynamically favoured (ΔG = −1.7 kcal mol^{-1} in CH_2Cl_2 and −6.0 kcal mol^{-1} in water). The details of the computational method are reported in ESI-CD (p. S2†).

Scope of the reaction

With the optimised reaction conditions in hand, we tested this new catalytic protocol with several alkenes demonstrating its wide applicability and its tolerance towards a plethora of functional groups with different electronic properties. The results are reported in Table 2. Reactions were carried out both on 0.5 and 1 mmol scales with no meaningful differences in the outcome. For instance, olefins with different chain lengths were tested and the best results were observed with hexadec-1-ene **1a** and oct-1-ene **1c**, which both afforded the corresponding sulfones **3a** and **3c** in 80% yields. Slightly lower yields were observed with dodec-1-ene **1b** (**3b**, 66%), pent-1-ene **1d** (**3d**, 57%) and with cyclohexene **1f** (**3f**, 50%). Remarkably, ethylene **1e** could also be employed at atmospheric pressure, affording sulfone **3e** in a 40% yield. As shown in Table 2, our methodology was successfully applied to many functionalised olefins producing a library of substituted sulfones. Leaving groups and protic groups (respectively –Br and –OH) were tolerated, as demonstrated in the case of 4-bromobut-1-ene **1g** which produced the corresponding sulfone **3g** in a very good yield, both when 0.5 and 1 mmol of **1g** were used (69 and 79%, respectively). The same was observed with but-3-en-1-ol (**1h**) and hex-5-en-1-ol (**1i**), whose corresponding sulfones **3h** and **3i** were obtained in 78 and 90% yields, respectively. Interestingly, sulfone **3i** was achieved in a higher yield than that reported by Yu[25] applying iridium photocatalysis (90% *versus* 69% yield). An

Table 2 Scope of the hydrosulfonylation reaction with alkenes[a,b]

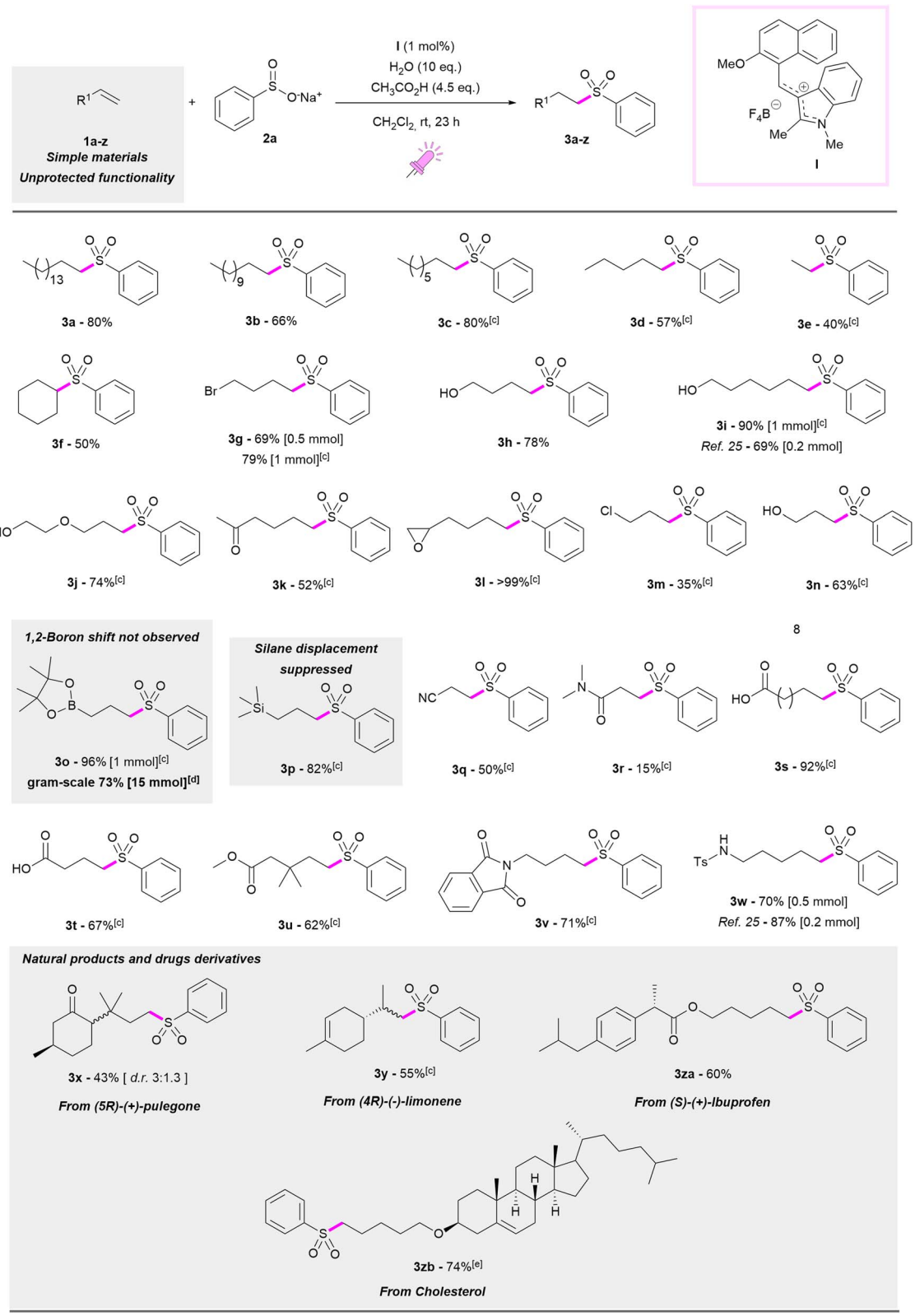

[a] Reaction conditions: alkene **1a–z** (0.5 mmol), sodium benzenesulfinate **2a** (1.6 eq.), **I** (1 mol%), in CH_2Cl_2 (2.5 mL, 0.2 M), CH_3COOH (4.5 eq.), H_2O (10 eq.), 40W Kessil purple LED lamp (390 nm), 23 h, room temperature. [b] Yield determined on the isolated product. [c] Reaction carried out on 1 mmol of **1c–e**, **1g**, **1i–v** and **1y** in 5 mL of CH_2Cl_2. [d] Reaction scaled up to 15 mmol of **1o**. [e] Reaction time 46 h for **1zb**.

ether functional group was also tolerated, with 2-allyloxyethanol **1j** delivering the corresponding sulfone **3j** in a 74% yield. Ketones and epoxy rings were easily introduced onto the sulfone product as shown in the case of hex-1-en-2-one **1k** and of 5,6-epoxyhex-1-ene **1l** (52% yield for **3k**, quantitative yield for **3l**). Our strategy can be also applied to α,β-unsaturated enals or enones, but it did not prove to be advantageous compared to the polar protocol affording the corresponding β-sulfonyl-ketones or aldehydes in lower yields. Considering alkenes functionalised at the allylic position, the formation of the sulfone product can be directly correlated to the leaving-group nature of the substituent. For allyl bromide, only (allylsulfonyl)benzene, which was derived from nucleophilic displacement, was produced. However, allyl chloride **1m**, produced the corresponding ((3-chloropropyl)sulfonyl)benzene **3m** in a 35% yield, because of the worse leaving ability of chloride than that of bromide, but still in the presence of 18% of (allylsulfonyl) benzene. The reaction was also successfully accomplished with allyl alcohol **1n**, with the corresponding phenylsulfonylpropan-1-ol **3n** produced in 63% yield. Interestingly, the nucleophilic displacement was totally suppressed with allylboronic acid pinacol ester **1o** and allyltrimethylsilane **1p**. Sulfone **3o** was obtained in an excellent 96% yield. This is a remarkable result considering that allylboronic esters and allyl silanes can be exploited as allylation reagents where boronic ester or silane moieties get lost or 1,2-boron migration is observed.[53–56] Considering the high synthetic value of compound **3o** as a possible substrate for a Suzuki coupling, we scaled-up its

Table 3 Scope of the hydrosulfonylation reaction with sulfinates [a,b]

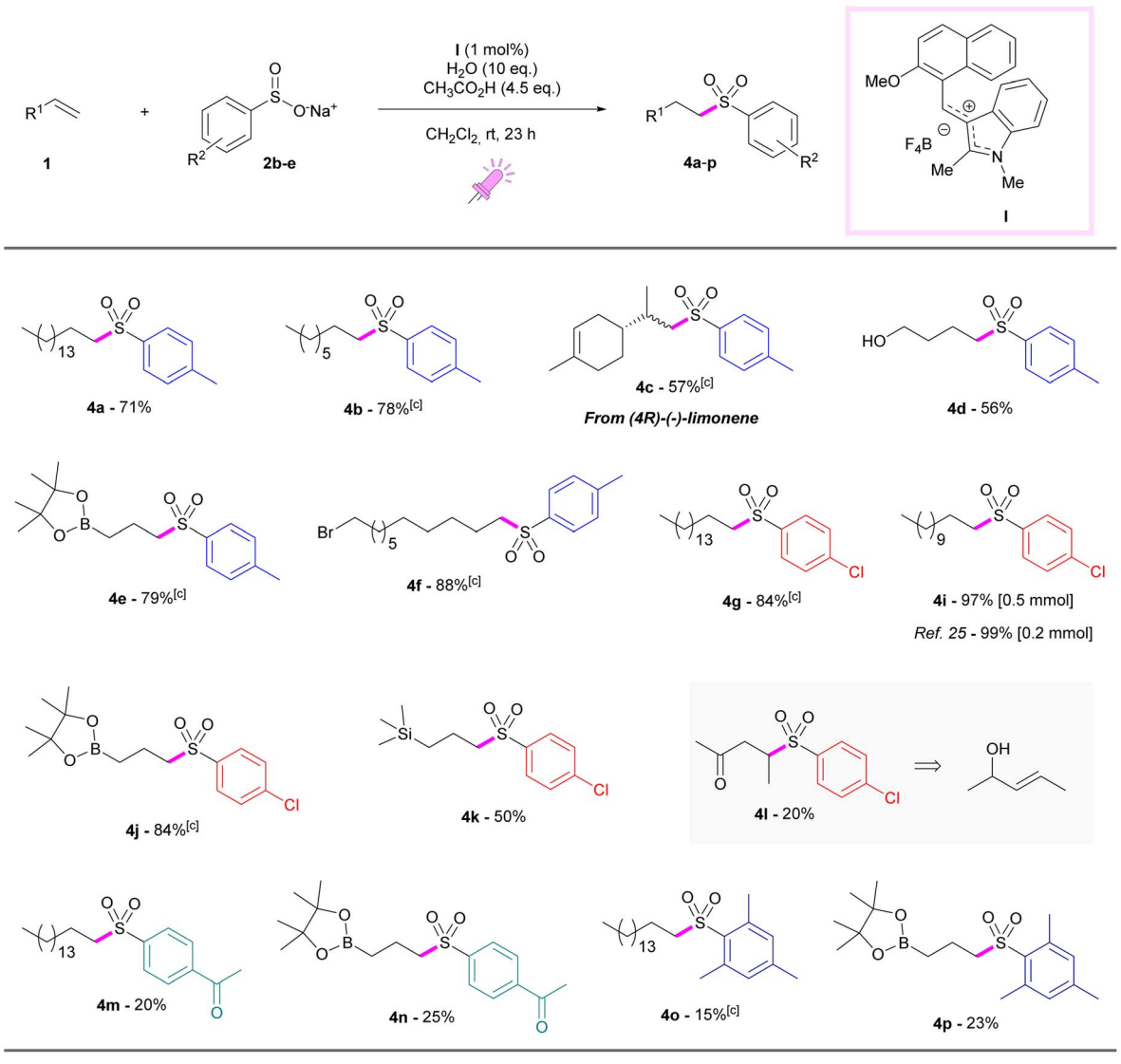

[a] Reaction conditions: alkene **1** (0.5 mmol), sodium aryl sulfinates **2b–e** (1.6 eq.), **I** (1 mol%), in CH_2Cl_2 (2.5 mL, 0.2 M), CH_3COOH (4.5 eq.), H_2O (10 eq.), 40W Kessil purple LED lamp (390 nm), 23 h, room temperature. [b] Yield determined on the isolated product. [c] Reaction carried out on 1 mmol of alkenes **1b–c**, **1e–g**, **1j** and **1o** in 5 mL of CH_2Cl_2.

synthesis to 15 mmol with a yield of 73% (see the ESI† for pictures of the reaction work flow for large scale sulfonylation). The use of **1p** was also successful with sulfone **3p** produced in 82% yield. Taking into account polymerization as a side reaction associated with acrylonitrile **1q**, 3-(phenylsulfonyl)propanenitrile **3q** was obtained in a satisfactory 50% yield. However, when *N*,*N*-dimethylacrylamide **1r** was used as the reagent, a drop in yield to 15% for **3r** was observed. Moreover, carboxylic acid (**1s–t**) or ester (**1u**) moieties were very well tolerated, with the isolation of the corresponding sulfones **3s**, **3t** and **3u**, respectively in 92, 67 and 62% yields. Masked amine functionality could be easily introduced from 4-phtalimidobut-1-ene **1v** (71% for **3v**). A similar result was observed when a tosylamine was incorporated in the starting alkene with the product **3w** produced in 70% yield. Styrenes were also tested, but no sulfonylation product was obtained. Finally, the hydrosulfonylation protocol was validated on natural and biologically active molecules. (5*R*)-(+)-Pulegone derivative **1x** produced the corresponding product **3x** in a 43% yield as a diastereomeric mixture in a 3 : 1.3 ratio. Remarkably, (4*R*)-(−)-limonene **1y** afforded the product **3y** with complete selectivity to the terminal double bond. Hydrosulfonylated analogues of (*S*)-(+)-Ibuprofen and cholesterol derivatives were isolated in good yields (60% for **3za** and 74% for **3zb**, respectively). In order to obtain the full conversion of **1zb**, the reaction time was increased to 46 h (35% yield for **3zb** after 23 h).

The scope of the sulfinate was then studied, and sodium 4-methylbenzenesulfinate **2b** was first applied affording the products **4a–f** in good to excellent yields, comparable to those obtained with sodium benzenesulfinate **2a**. Sulfones **4a** and **4b** were obtained by reaction with hexadec-1-ene **1a** and oct-1-ene **1c** in 71 and 78% yield, respectively. Also in the case of (4*R*)-(−)-limonene **1w** the outcome was comparable to that of sulfinate **2a** (57% *vs.* 55%) with a complete selectivity toward the less hindered double bond. Actually, simple alkenes successfully reacted with all the substituted sulfinates. Hexadec-1-ene **1a**, for example, afforded sulfone **4g** in 84% yield after reaction with sodium 4-chlorobenzenesulfinate **1c**. The shorter alkene **1c** gave sulfone **4i** in nearly quantitative yield (97%). In the case of sodium 4-acetylbenzenesulfinate **1d** and the sterically hindered mesityl sulfinate **1e** a drop in yield was obtained (**4m**, 20% and **4o**, 15%). Sulfone **4f**, derived from 11-bromoundec-1-ene **1aa** and *p*-tolylsulfinate **2b**, was produced in 88% yield thus confirming the compatibility of this protocol with alkyl bromides. But-3-enol **1h** successfully reacted with **2b** (**4d**, 56%), with a lower efficiency than **2a**. The hydrosulfonylation of allylpinacolborane **1n** was successfully performed with several sulfinates (see Table 3, products **4e**, 79% and **4j** 84% yield). Anyway, a marked decrease in yield was observed in the case of sulfinates **2d** and **2e** (**4n** and **4p**, 23 and 25% yield, respectively), consistent with the results obtained with the same sulfinates with other alkenes, as previously described. Sulfone **4k** was isolated in 50% yield by the reaction of allyltrimethylsilane **1o** and *p*-Cl-sulfinate **2c** thus confirming a higher efficiency of **2a** with respect to other derivatives. Interestingly product **4l** bearing a ketone functionality, although in low yield, was obtained from 3-penten-2-ol **1ab** after a rearrangement.

Conclusions

In summary, we have developed a general light mediated hydrosulfonylation of unactivated alkenes using substituted aryl sulfinates in the presence of diarylmethylium tetrafluoroborates. These salts, which are cheap, stable under air and easily prepared on a multigram scale, were employed for the first time in a photoredox process with the same loading of iridium-based photocatalysts. This methodology, which is operationally simple and do not require anhydrous conditions, allowed the access to more than 40 functionalised sulfones with a remarkable functional group tolerance and scalability up to 15 mmol. Natural products and biologically active molecules were hydrosulfonylated under mild reaction conditions. Experimental and computational mechanistic studies revealed that the key sulfonyl radical can be formed through an innovative mechanism involving a photoactive adduct derived from the diarylmethylium salt and the sulfinate upon interaction with light. A PCET process is then exploited to restore the catalytic species.

Data availability

The data, both experimental and computational, that supports the findings of this study are available in the ESI of this article.†

Author contributions

All authors have given approval to the final version of the manuscript. The manuscript was written through contributions of all authors. Polyssena Renzi (conceptualization, methodology, investigation, visualization, writing – original draft, writing review and editing), Emanuele Azzi, Sylvain Ascensio, Stefano Parisotto, Fabrizio Sordello, and Francesco Pellegrino (investigation, writing review and editing), Giovanni Ghigo (investigation, software, writing – original draft, writing review and editing), and Annamaria Deagostino (conceptualization, funding acquisition, project administration, supervision, writing – original draft, writing – review & editing).

Conflicts of interest

There are no conflicts to declare.

Acknowledgements

This work is dedicated to Dr Margherita Barbero on the occasion of her retirement. This work was supported by MIUR (Ministero dell'Istruzione, dell'Università e della Ricerca).

References

1 M. Feng, B. Tang, S. H. Liang and X. Jiang, Sulfur Containing Scaffolds in Drugs: Synthesis and Application in Medicinal Chemistry, *Curr. Top. Med. Chem.*, 2016, **16**, 1200–1216.

2 K. A. Scott and J. T. Njardarson, Analysis of US FDA-Approved Drugs Containing Sulfur Atoms, *Curr. Top. Med. Chem.*, 2018, **376**, 5.
3 D. Joseph, M. A. Idris, J. Chen and S. Lee, Recent Advances in the Catalytic Synthesis of Arylsulfonyl Compounds, *ACS Catal.*, 2021, **11**, 4169–4204.
4 S. Liang, K. Hofman, M. Friedrich, J. Keller and G. Manolikakes, Recent Progress and Emerging Technologies towards a Sustainable Synthesis of Sulfones, *ChemSusChem*, 2021, **14**, 4878–4902.
5 B. M. Trost and D. P. Curran, Chemoselective oxidation of sulfides to sulfones with potassium hydrogen persulfate, *Tetrahedron Lett.*, 1981, **22**, 1287–1290.
6 W. Su, An efficient method for the oxidation of sulfides to sulfones, *Tetrahedron Lett.*, 1994, **35**, 4955–4958.
7 S. Hussain, S. K. Bharadwaj, R. Pandey and M. K. Chaudhuri, Borax-Catalyzed and pH-Controlled Selective Oxidation of Organic Sulfides by H_2O_2: An Environmentally Clean Protocol, *Eur. J. Org. Chem.*, 2009, **2009**, 3319–3322.
8 K. Bahrami, M. M. Khodaei and M. Sheikh Arabi, TAPC-Promoted Oxidation of Sulfides and Deoxygenation of Sulfoxides, *J. Org. Chem.*, 2010, **75**, 6208–6213.
9 S. Ye, G. Qiu and J. Wu, Inorganic sulfites as the sulfur dioxide surrogates in sulfonylation reactions, *Chem. Commun.*, 2019, **55**, 1013–1019.
10 G. Qiu, K. Zhou and J. Wu, Recent advances in the sulfonylation of C–H bonds with the insertion of sulfur dioxide, *Chem. Commun.*, 2018, **54**, 12561–12569.
11 S. Ye, M. Yang and J. Wu, Recent advances in sulfonylation reactions using potassium/sodium metabisulfite, *Chem. Commun.*, 2020, **56**, 4145–4155.
12 A. Lanfranco, R. Moro, E. Azzi, A. Deagostino and P. Renzi, Unconventional approaches for the introduction of sulfur-based functional groups, *Org. Biomol. Chem.*, 2021, **19**, 6926–6957.
13 L. Wu, L. Peng, Z. Hu, Y. Jiao and Z. Tang, Recent Advances of Sulfonylation Reactions in Water, *Curr. Org. Synth.*, 2020, **17**, 271–281.
14 E. Azzi, A. Lanfranco, R. Moro, A. Deagostino and P. Renzi, Visible light as the key for the formation of carbon-sulfur bonds in sulfones, thioethers, and sulfonamides: An update, *Synthesis*, 2021, **53**, 3440–3468.
15 Z. Lu, M. Shang and H. Lu, Organic Sulfinic Acids and Salts in Visible Light-Induced Reactions, *Synthesis*, 2022, **54**(5), 1231–1249.
16 D.-Q. Dong, Q.-Q. Han, S.-H. Yang, J.-C. Song, N. Li, Z.-L. Wang and X.-M. Xu, Recent Progress in Sulfonylation *via* Radical Reaction with Sodium Sulfinates, Sulfinic Acids, Sulfonyl Chlorides or Sulfonyl Hydrazides, *ChemistrySelect*, 2020, **5**, 13103–13134.
17 O. M. Mulina, A. I. Ilovaisky, V. D. Parshin and A. O. Terent'ev, Oxidative Sulfonylation of Multiple Carbon-Carbon bonds with Sulfonyl Hydrazides, Sulfinic Acids and their Salts, *Adv. Synth.Catal.*, 2020, **362**, 4579–4654.
18 X. Ye, X. Wu, S.-r. Guo, D. Huang and X. Sun, Recent advances of sodium sulfinates in radical reactions, *Tetrahedron Lett.*, 2021, **81**, 153368.
19 B. Ni, B. Zhang, J. Han, B. Peng, Y. Shan and T. Niu, Heterogeneous carbon nitrides photocatalysis multicomponent hydrosulfonylation of alkynes to access β-keto sulfones with the insertion of sulfur dioxide in aerobic aqueous medium, *Org. Lett.*, 2020, **22**, 670–674.
20 X. Du, J.-S. Zhen, X.-H. Xu, H. Yuan, Y.-H. Li, Y. Zheng, C. Xue and Y. Luo, Hydrosulfonylation of Alkenes with Sulfonyl Imines *via* Ir/Cu Dual Photoredox Catalysis, *Org. Lett.*, 2022, **24**, 3944–3949.
21 A. Hossain, S. Engl, E. Lutsker and O. Reiser, Visible-Light-Mediated Regioselective Chlorosulfonylation of Alkenes and Alkynes: Introducing the Cu(II) Complex $[Cu(dap)Cl_2]$ to Photochemical ATRA Reactions, *ACS Catal.*, 2019, **9**, 1103–1109.
22 M. Alkan-Zambada and X. Hu, Cu-Catalyzed Photoredox Chlorosulfonation of Alkenes and Alkynes, *J. Org. Chem.*, 2019, **84**, 4525–4533.
23 S. K. Pagire, S. Paria and O. Reiser, Synthesis of β-Hydroxysulfones from Sulfonyl Chlorides and Alkenes Utilizing Visible Light Photocatalytic Sequences, *Org. Lett.*, 2016, **18**, 2106–2109.
24 X.-J. Tang and W. R. Dolbier Jr, Efficient Cu-catalyzed Atom Transfer Radical Addition Reactions of Fluoroalkylsulfonyl Chlorides with Electron-deficient Alkenes Induced by Visible Light, *Angew. Chem., Int. Ed.*, 2015, **54**, 4246–4249.
25 J. J. Wang and W. Yu, Hydrosulfonylation of Unactivated Alkenes by Visible Light Photoredox Catalysis, *Org. Lett.*, 2019, **21**, 9236–9240.
26 Y. Zheng, Y. You, Q. Shen, J. Zhang, L. Liu and X.-H. Duan, Visible-light-induced anti-Markovnikov hydrosulfonation of styrene derivatives, *Org. Chem. Front.*, 2020, **7**, 2069–2074.
27 Y. Chen, N. McNamara, O. May, T. Pillaiyar, D. C. Blakemore and S. V. Ley, Photoredox Generation of Sulfonyl Radicals and Coupling with Electron Deficient Olefins, *Org. Lett.*, 2020, **22**, 5746–5748.
28 S. M. Hell, C. F. Meyer, A. Misale, J. B. I. Sap, K. E. Christensen, M. C. Willis, A. A. Trabanco and V. Gouverneur, Hydrosulfonylation of Alkenes with Sulfonyl Chlorides under Visible Light Activation, *Angew. Chem., Int. Ed.*, 2020, **59**, 11620–11626.
29 T. Föll, J. Rehbein and O. Reiser, Ir(ppy)3-Catalyzed, Visible-Light-Mediated Reaction of α-Chloro Cinnamates with Enol Acetates: An Apparent Halogen Paradox, *Org. Lett.*, 2018, **20**, 5794–5798.
30 Britannica, The Editors of Encyclopaedia, *iridium*, Encyclopedia Britannica, 29 Jan. 2021, **https://www.britannica.com/science/iridium**, accessed 20 March 2022.
31 A. Joshi-Pangu, F. Lévesque, H. G. Roth, S. F. Oliver, L.-C. Campeau, D. Nicewicz and D. A. DiRocco, Acridinium-Based Photocatalysts: A Sustainable Option in Photoredox Catalysis, *J. Org. Chem.*, 2016, **81**, 7244–7249.
32 J. Cervantes-González, D. A. Vosburg, S. E. Mora-Rodriguez, M. A. Vázquez, L. G. Zepeda, C. Villegas Gómez and

S. Lagunas-Rivera, Anthraquinones: Versatile Organic Photocatalysts, *ChemCatChem*, 2020, **12**, 3811–3827.

33 Y. Lee and M. S. Kwon, Emerging Organic Photoredox Catalysts for Organic Transformations, *Eur. J. Org. Chem.*, 2020, **2020**, 6028–6043.

34 V. Srivastava and P. P. Singh, Eosin y catalysed photoredox synthesis: A review, *RSC Adv.*, 2017, **7**, 31377–31392.

35 N. A. Romero and D. A. Nicewicz, Organic Photoredox Catalysis, *Chem. Rev.*, 2016, **116**, 10075–10166.

36 C. Pezzetta, A. Folli, O. Matuszewska, D. Murphy, R. W. M. Davidson and D. Bonifazi, peri-Xanthenoxanthene (PXX): a Versatile Organic Photocatalyst in Organic Synthesis, *Adv. Synth. Catal.*, 2021, **363**, 4740–4753.

37 P. Renzi, E. Azzi, E. Bessone, G. Ghigo, S. Parisotto, F. Pellegrino and A. Deagostino, Blue light enhanced Heck arylation at room temperature applied to allenes, *Org. Chem. Front.*, 2022, **9**, 906–916.

38 E. Azzi, G. Ghigo, S. Parisotto, F. Pellegrino, E. Priola, P. Renzi and A. Deagostino, Visible Light Mediated Photocatalytic *N*-Radical Cascade Reactivity of γ,δ-Unsaturated *N*-Arylsulfonylhydrazones: A General Approach to Structurally Diverse Tetrahydropyridazines, *J. Org. Chem.*, 2021, **86**, 3300–3323.

39 S. Parisotto, G. Garreffa, C. Canepa, E. Diana, F. Pellegrino, E. Priola, C. Prandi, V. Maurino and A. Deagostino, Visible-Light-Driven Photocatalytic Transformation of α,β-Unsaturated-N-Tosylhydrazones: A Novel Route to Allylic Sulfones, *ChemPhotoChem*, 2017, **1**, 56–59.

40 N. Armenise, S. Dughera, A. Gualandi, L. Mengozzi, M. Barbero and P. G. Cozzi, Organocatalyzed Asymmetric Alkylation of Stable Aryl or Heteroaryl(3-indolyl)methylium o-Benzenedisulfonimides, *Asian J. Org. Chem.*, 2015, **4**, 337–345.

41 M. Barbero, R. Buscaino, S. Cadamuro, S. Dughera, A. Gualandi, D. Marabello and P. G. Cozzi, Synthesis of Bench-Stable Diarylmethylium Tetrafluoroborates, *J. Org. Chem.*, 2015, **80**, 4791–4796.

42 M. Barbero, S. Cadamuro, F. Cauda, S. Dughera, G. Gervasio and P. Venturello, Preparation and Characterization of Aryl or Heteroaryl(3-indolyl)methylium o-Benzenedisulfonimides, *J. Org. Chem.*, 2012, **77**, 4278–4287.

43 M. Barbero, S. Cadamuro, S. Dughera, G. Ghigo, D. Marabello and P. Morgante, Efficient alkylation of cyclic silyl enol ethers by diarylmethylium salts, *Tetrahedron Lett.*, 2016, **57**, 4758–4762.

44 R. J. Mayer, N. Hampel, P. Mayer, A. R. Ofial and H. Mayr, Synthesis, Structure, and Properties of Amino-Substituted Benzhydrylium Ions – A Link between Ordinary Carbocations and Neutral Electrophiles, *Eur. J. Org. Chem.*, 2019, **2019**, 412–421.

45 R. J. Mayer, A. R. Ofial, H. Mayr and C. Y. Legault, Lewis Acidity Scale of Diaryliodonium Ions toward Oxygen, Nitrogen, and Halogen Lewis Bases, *J. Am. Chem. Soc.*, 2020, **142**, 5221–5233.

46 On a relative molar scale, diarylcarbenium salt I is more than three hundred times cheaper than [Ir(dF(CF3)ppy)2(dtbbpy)] PF6. For the calculation of diarylcarbenium salt I cost and comparison with prices of iridium catalysts see the ESI†

47 K. Kohara, A. Trowbridge, M. A. Smith and M. J. Gaunt, Thiol-Mediated α-Amino Radical Formation *via* Visible-Light-Activated Ion-Pair Charge-Transfer Complexes, *J. Am. Chem. Soc.*, 2021, **143**, 19268–19274.

48 D. R. Weinberg, C. J. Gagliardi, J. F. Hull, C. F. Murphy, C. A. Kent, B. C. Westlake, A. Paul, D. H. Ess, D. G. McCafferty and T. J. Meyer, Proton-Coupled Electron Transfer, *Chem. Rev.*, 2012, **112**, 4016–4093.

49 R. Tyburski, T. Liu, S. D. Glover and L. Hammarström, Proton-Coupled Electron Transfer Guidelines, Fair and Square, *J. Am. Chem. Soc.*, 2021, **143**, 560–576.

50 R. G. Agarwal, S. C. Coste, B. D. Groff, A. M. Heuer, H. Noh, G. A. Parada, C. F. Wise, E. M. Nichols, J. J. Warren and J. M. Mayer, Free Energies of Proton-Coupled Electron Transfer Reagents and Their Applications, *Chem. Rev.*, 2022, **122**, 1–49.

51 P. R. D. Murray, J. H. Cox, N. D. Chiappini, C. B. Roos, E. A. McLoughlin, B. G. Hejna, S. T. Nguyen, H. H. Ripberger, J. M. Ganley, E. Tsui, N. Y. Shin, B. Koronkiewicz, G. Qiu and R. R. Knowles, Photochemical and Electrochemical Applications of Proton-Coupled Electron Transfer in Organic Synthesis, *Chem. Rev.*, 2022, **122**, 2017–2291.

52 T. F. Markle, J. W. Darcy and J. M. Mayer, A new strategy to efficiently cleave and form C–H bonds using proton-coupled electron transfer, *Sci. Adv.*, 2018, **4**, eaat5776.

53 R. Wada, K. Oisaki, M. Kanai and M. Shibasaki, Catalytic Enantioselective Allylboration of Ketones, *J. Am. Chem. Soc.*, 2004, **126**, 8910–8911.

54 S. E. Denmark and J. Fu, Catalytic Enantioselective Addition of Allylic Organometallic Reagents to Aldehydes and Ketones, *Chem. Rev.*, 2003, **103**, 2763–2794.

55 M. Berger, D. Carboni and P. Melchiorre, Photochemical Organocatalytic Regio- and Enantioselective Conjugate Addition of Allyl Groups to Enals, *Angew. Chem., Int. Ed.*, 2021, **60**, 26373–26377.

56 K. Jana and A. Studer, Allylboronic Esters as Acceptors in Radical Addition, Boron 1,2-Migration, and Trapping Cascades, *Org. Lett.*, 2022, **24**, 1100–1104.